Codebook Design for Wideband FDD Massive MIMO Hybrid Precoding

Muhammad Salman Al Faruq, Danish Mehmood Mughal, Min Young Chung, Sang-Hyo Kim

Department of Electrical and Computer Engineering

Sungkyunkwan University

Suwon, South Korea

Email: iamshkim@skku.edu

Abstract—Obtaining accurate CSI in frequency division duplexing (FDD) systems is a challenging problem due to the extensive feedback overhead. Applying a precoder to the CSI reference signal (CSI-RS) reduces feedback overhead and improves the reception of the CSI-RS. However, fully digital precoding dedicates RF chains for each antenna, which makes massive MIMO with a large antenna array expensive. Hybrid precoding has attracted increasing interest as a practical solution that reduces the number of RF chains. Operating in analog and digital domains introduces additional constraints on the design of the precoder. In this paper, we propose a codebook design for wideband FDD massive MIMO hybrid precoding systems. We formulate the precoding design problem as a sparsityconstrained matrix reconstruction problem. Using orthogonal matching pursuit (OMP), we develop a wideband precoding algorithm that approximates unconstrained partial channel reciprocity precoding using a smaller number of RF chains than the total number of antennas. We present simulation results that exhibit the hybrid precoding shows a slight performance gap compared to unconstrained precoding.

Index Terms—Massive MIMO, FDD, hybrid precoding, compressive sensing

I. INTRODUCTION

With the global deployment of 5G networks, research has already shifted toward the development of sixth-generation (6G) wireless systems. 6G is envisioned to support immersive services such as extended reality (XR), holographic communications, and large-scale Internet of Things (IoT), while achieving targets like sub-millisecond latency, terabit-per-second data rates, and native integration of sensing and communications [1], [2]. These ambitious goals have stimulated extensive research across various scenarios, including new approaches to channel coding [3]–[5], reliability enhancement for mission-critical services [6], [7], and efficient spectrum utilization [8], [9]. Among these efforts, massive MIMO continues to play a central role, providing the foundation for meeting 6G performance requirements. Massive MIMO improves data rates through increased spectral efficiency. The improvement

This work was partly supported by Institute of Information & communications Technology Planning & Evaluation (IITP) grant funded by the Korea government (MSIT) Development of 3D Spatial Mobile Communication Technology (2021-0-00794), Development of the Upper-mid Band Extreme massive MIMO (RS-2024-00397216), and Network Research Center: Advanced Channel Coding and Channel Estimation Technologies for Wireless Communication Evolution (RS-2024-00398449). (Corresponding author: Sang-Hyo Kim.)

is enabled by the beamforming, interference rejection, and spatial multiplexing capabilities of massive MIMO [10]. The downlink (DL) channel state information (CSI) at the base station (BS) is crucial to perform these massive MIMO capabilities. Initially, massive MIMO was designed in a time division duplexing (TDD) system [11]. Relying on channel reciprocity, TDD massive MIMO systems eliminate the need for CSI feedback.

Frequency-division duplexing (FDD) wireless networks are still widely used in many existing systems and are expected to continue in the next generation. Unfortunately, FDD faces greater challenges due to the absence of full channel reciprocity. In this system, the user equipment (UE) needs to feed back DL CSI to the BS. The use of a large number of antennas in massive MIMO results in a significant feedback overhead. Therefore, CSI feedback in FDD massive MIMO becomes challenging.

Several research works have investigated methods to reduce the significant overhead of CSI feedback in FDD massive MIMO. The works in [12], [13] use the compressive sensing (CS) technique to compress the number of pilot training and feedback. The deep learning method has been proposed for solving the CSI feedback problem in [14]–[16]. Partial reciprocity in the angular domain and channel sparsity are utilized in other CSI feedback methods. BS can use the information of the channel covariance matrix (CCM) [17]–[19] and angle of departure (AoD) [20], [21] to reduce feedback overhead.

The large antenna array in a massive MIMO system also introduces high cost and power consumption when implemented using dedicated RF chains for each antenna or fully digital precoding. Hybrid precoding is a practical solution that reduces the number of RF chains by dividing precoding into two stages [22]. The digital precoding stage is performed in baseband processing, allowing for the flexibility to control the magnitude and phase of all subcarriers. Analog precoding in the RF domain is typically implemented using phase shifters, which introduce new hardware constraints for hybrid precoding. The analog precoder is common for all subcarriers, and all elements have a constant magnitude. The works in [17]–[21] do not address the high-cost implementation of a massive MIMO system. In terms of performance, the partial channel reciprocity codebook [19] outperforms the Rel-16 5G code-

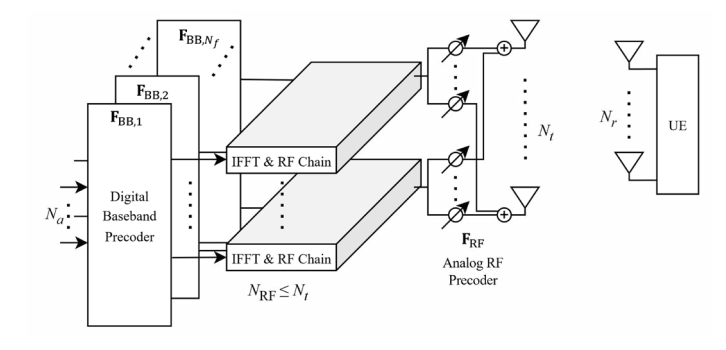


Fig. 1. A block diagram of an OFDM-based hybrid massive MIMO system.

book with lower overhead and higher received signal-to-noise ratio (SNR) of the CSI reference signal (CSI-RS). However, the partial-channel reciprocity codebook is not specialized in reducing the number of RF chains in massive MIMO.

The benefit of hybrid precoding motivates us to develop a codebook that works with a reduced number of RF chains while maintaining accurate CSI feedback. In this paper, we focus on designing codebooks for wideband FDD massive MIMO hybrid precoding. We first derive the unconstrained wideband FDD massive MIMO precoder based on the partial-channel reciprocity codebook. Then, we develop a wideband hybrid precoding algorithm to approximate the unconstrained precoder. The approximation is formulated as a sparsity-constrained matrix reconstruction problem, which is solved using orthogonal matching pursuit (OMP) by exploiting the limited scattering of the channel.

Notations: \mathbf{A} is a matrix; \mathbf{a} is a vector; a is a scalar; $\mathbf{A}^{(i)}$ is the i-th column of \mathbf{A} ; $[\mathbf{A}]_{i,j}$ is the element in the i-th row and the j-th column of matrix \mathbf{A} ; $(\cdot)^T$ and $(\cdot)^H$ denote transpose and conjugate transpose respectively; $\|\mathbf{A}\|_F$ is the Frobenius norm of \mathbf{A} and $\|\mathbf{a}\|_p$ denotes the p-norm of vector \mathbf{a} ; diag (\mathbf{A}) is a vector of diagonal elements of \mathbf{A} ; zeros(N,M) is a $N\times M$ zero matrix; \mathbf{I}_N is the $N\times N$ identity matrix; $\mathcal{CN}(\mathbf{a},\mathbf{A})$ is a complex Gaussian vector with mean \mathbf{a} and covariance matrix \mathbf{A} ; $\mathbb{E}\{\cdot\}$ denotes the expectation; $\mathbb{C}^{x\times y}$ denotes $x\times y$ complex space.

II. SYSTEM MODEL

Consider the OFDM-based CSI feedback system model in Fig. 1 where a single UE with N_r uniform linear array (ULA) antenna is connected to a BS with N_t antennas and $N_{\rm RF}$ RF chains. BS transmits N_a ports of the CSI reference signal (CSI-RS) multiplexed on multiple subcarriers such that $N_{\rm RF} \leq N_t$. The entire bandwidth is partitioned into N_f subbands, each consisting of a group of subcarriers.

The BS is assumed to use a single-polarization uniform planar array (UPA) on the yz plane with N_y and N_z elements on the y and z axes, respectively. The total number of BS antennas is $N_t = N_y N_z$. Denoting the azimuth of the departure angle (AOD) and the zenith of the departure angle

(ZOD) by φ_{AOD} and θ_{ZOD} , respectively, we can write the steering vector for this UPA antenna as

$$\mathbf{a}(\varphi,\theta) = \frac{1}{\sqrt{N_t}} [1, \dots, e^{j\frac{2\pi}{\lambda}d(m\sin\varphi\sin\theta + n\cos\theta)}, \dots, e^{j\frac{2\pi}{\lambda}d((N_y - 1)\sin\varphi\sin\theta + (N_z - 1)\cos\theta)}]^T, \quad (1)$$

where λ is the wavelength of the center frequency, and d is the spacing between the antenna elements. $0 < m < N_y - 1$ and $0 < n < N_z - 1$ are the y and z indices of an antenna element, respectively.

In the baseband, the reference signal in each subband $k=1,\cdots,N_f$ is precoded using the baseband precoder $\mathbf{F}_{\mathrm{BB},k}\in\mathbb{C}^{N_{\mathrm{RF}}\times N_a}$, then modulated into a signal in the time domain. In the time domain, the analog precoder $\mathbf{F}_{\mathrm{RF}}\in\mathbb{C}^{N_t\times N_{\mathrm{RF}}}$ is applied to the signal. Note that the analog precoder \mathbf{F}_{RF} is common for all subbands. The precoded baseband CSI-RS in the k-th subband is

$$\mathbf{x}_k = \mathbf{F}_{\mathrm{RF}} \mathbf{F}_{\mathrm{BB}} \, {}_k \mathbf{s}_k, \tag{2}$$

where $\mathbf{s}_k \in \mathcal{C}^{N_a \times 1}$ is the non-precoded CSI-RS in subband k, such that $\mathbb{E}[\mathbf{s}_k \mathbf{s}_k^H] = \frac{P}{KN_a} \mathbf{I}_{N_a}$, and P is the average total non-precoded CSI-RS power. Since the analog precoder \mathbf{F}_{RF} is implemented using a phase shifter, it has a constant modulus constraint $|[\mathbf{F}_{\mathrm{RF}}]_{i,j}|^2 = N_t^{-1}$. Denote the channel matrix in subband k as $\mathbf{H}_k(t) \in \mathbb{C}^{N_r \times N_t}$, and the received signal at subband k can be expressed as

$$\mathbf{y}_k(t) = \mathbf{H}_k(t)\mathbf{F}_{RF}\mathbf{F}_{BB,k}\mathbf{s}_k + \mathbf{n}_k(t), \tag{3}$$

where $\mathbf{n}_k(t) \sim \mathcal{CN}(\mathbf{0}, \sigma_n^2 \mathbf{I}_{N_r})$ is the additive white Gaussian noise (AWGN) with noise variance σ_n^2 .

The hybrid precoder for all subbands can be concatenated into the overall hybrid precoding matrix $\mathbf{W} \in \mathbb{C}^{N_a \times N_t N_f}$ as

$$\mathbf{W} = \begin{bmatrix} \mathbf{F}_{RF} \mathbf{F}_{BB,1} \\ \mathbf{F}_{RF} \mathbf{F}_{BB,2} \\ \vdots \\ \mathbf{F}_{RF} \mathbf{F}_{BB,N_f} \end{bmatrix}^{T}$$
(4)

The row of the overall hybrid precoding matrix $\mathbf{W}_n \in \mathbb{C}^{1 \times N_t N_f}$ for a port $n=1,\cdots,N_a$ is assumed to have a unit norm $||\mathbf{W}_n||=1$. Similar to the partial channel reciprocity codebook [19], the UE performs a summation of the received signal in the frequency domain as

$$\mathbf{y}(t) = \sum_{k=1}^{N_f} \mathbf{y}_k(t) \tag{5}$$

$$= \mathbf{sW}\underline{\mathbf{H}}(t) + \mathbf{n}(t) \tag{6}$$

where

$$\mathbf{s} = \sum_{k=1}^{N_f} \mathbf{s}_k^T,\tag{7}$$

$$\mathbf{n}(t) = \sum_{k=1}^{N_f} \mathbf{n}_k^T(t). \tag{8}$$

and $\mathbf{H}(t) \in \mathbb{C}^{N_t N_f \times N_r}$ is the concatenated wideband channel:

$$\underline{\mathbf{H}}(t) = \left[\mathbf{H}_1(t), \mathbf{H}_2(t), \dots, \mathbf{H}_{N_f}(t)\right]^T. \tag{9}$$

The effective channel matrix $\mathbf{G}(t) \in \mathbb{C}^{N_a \times N_r}$ is defined as

$$\mathbf{G}(t) = \mathbf{W}\underline{\mathbf{H}}(t). \tag{10}$$

The UE then obtains the estimate of the effective channel $\hat{\mathbf{G}}(t)$ based on the non-precoded reference signal s, and feeds back the estimated vector to the BS. BS estimates DL CSI using information from the estimated effective channel $\hat{\mathbf{G}}(t)$ and the overall hybrid precoding matrix \mathbf{W} as

$$\underline{\hat{\mathbf{H}}}(t) = \mathbf{W}^H \hat{\mathbf{G}}(t). \tag{11}$$

III. CODEBOOK DESIGN

This section presents a CSI feedback method for the system shown in Fig. 1. First, we derived the unconstrained codebook based on the partial reciprocity channel. We then develop a wideband hybrid precoding algorithm to approximate the unconstrained codebook using OMP.

A. Unconstrained Codebook

The angular reciprocity properties of the FDD channel allow the estimation of the DL CCM through the projection method in a Hilbert space [23]. The joint spatial-frequency CCM is defined as

$$\mathbf{R} = \mathbb{E}\left\{ (\underline{\mathbf{H}}(t))(\underline{\mathbf{H}}(t))^{H} \right\}. \tag{12}$$

We assumed that this covariance matrix is available for codebook design. The conversion from uplink to downlink CCM is enabled by the partial reciprocity properties. The partial reciprocity codebook exploits the low-rank property of the CCM to reduce the amount of feedback overhead [19]. The set of precoders for the codebook is derived from the dominant eigenvectors obtained through eigenvalue decomposition of the channel covariance matrix. The eigenvalue decomposition can be written as

$$\mathbf{R} = \mathbf{U}\mathbf{\Sigma}\mathbf{U}^H,\tag{13}$$

where U is a matrix of eigenvectors of R:

$$\mathbf{U} = \left[\mathbf{u}_1, \mathbf{u}_2, \dots, \mathbf{u}_{N_t N_f}\right]. \tag{14}$$

Each eigenvector in \mathbf{U} corresponds to an eigenvalue ordered from the largest value in the diagonal entries of the diagonal matrix $\mathbf{\Sigma}$. The low-rank property of the covariance matrix \mathbf{R} indicates that signal paths with significant power are only transmitted in limited directions. The eigenvectors and eigenvalues represent the directions and the powers, respectively. We select the N_a eigenvectors with the highest eigenvalues from the matrix \mathbf{U} as

$$\mathbf{W}^{\text{UC}} = \begin{bmatrix} \mathbf{u}_1^H \\ \mathbf{u}_2^H \\ \vdots \\ \mathbf{u}_{N_a}^H \end{bmatrix} . \tag{15}$$

The unconstrained precoding matrix $\mathbf{W}^{\mathrm{UC}} \in \mathbb{C}^{N_a \times N_t N_f}$ can be applied to CSI-RS by OFDM precoding fully in

the digital domain. The unconstrained precoding matrix has the flexibility to control the magnitude and phase of the signal in the digital domain. We can rewrite the unconstrained precoding matrix \mathbf{W}^{UC} as

$$\mathbf{W}^{\mathrm{UC}} = \begin{bmatrix} \mathbf{F}_{1}^{\mathrm{UC}} \\ \mathbf{F}_{2}^{\mathrm{UC}} \\ \vdots \\ \mathbf{F}_{N_{f}}^{\mathrm{UC}} \end{bmatrix}^{T} . \tag{16}$$

where $\mathbf{F}_k^{\text{UC}} \in \mathbb{C}^{N_t \times N_a}$ is the unconstrained precoder matrix for subband k.

B. Codebook Design for Hybrid Precoding

The hybrid precoding design is subject to the following system constraints:

- 1) $N_{RF} \leq N_t$,
- 2) The analog precoder \mathbf{F}_{RF} is common for all subbands, and
- 3) $|[\mathbf{F}_{RF}]_{i,j}|^2 = N_t^{-1}$.

Based on these constraints, we design a hybrid precoder that approximates the unconstrained precoder and satisfies the constraints. The approximation problem can be written as

$$\underset{\mathbf{F}_{RF}, \{\mathbf{F}_{BB,k}\}_{k=1}^{N_f}}{\min} \sum_{k=1}^{N_f} \left\| \mathbf{F}_k^{UC} - \mathbf{F}_{RF} \mathbf{F}_{BB,k} \right\|_F, \qquad (17)$$
s.t.
$$\mathbf{F}_{RF} \in \mathcal{F}_{RF}, \\
\sum_{k=1}^{N_f} \left\| \mathbf{F}_{RF} \mathbf{F}_{BB,k} \right\|_F^2 \le \sum_{k=1}^{N_f} \left\| \mathbf{F}_k^{UC} \right\|_F^2,$$

where \mathcal{F}_{RF} is the set of feasible RF precoders, i.e., the set of matrices with constant magnitude entries. The problem is to find \mathbf{F}_{RF} and $\{\mathbf{F}_{BB,k}\}_{k=1}^{N_f}$ that minimizes the sum of the Frobenius norm of difference between the unconstrained precoder \mathbf{F}_k^{UC} and $\mathbf{F}_{RF}\mathbf{F}_{BB,k}$ for the entire N_f subband. This approximation is reasonable for designing the hybrid precoder [24].

The simple way to find a vector to build the analog precoder \mathbf{F}_{RF} is by selecting N_{RF} vectors from a set of steering vectors. A steering vector $\mathbf{a}(\varphi,\theta)$ satisfies the constraint of a constant modulus $|[\mathbf{F}_{\mathrm{RF}}]_{i,j}|^2 = N_t^{-1}$. We sample the steering vector angles (φ_l,θ_l) uniformly from the 3D space where $l=1,\ldots,N_{dict}$ and N_{dict} is the total number of steering vector samples in the directions. The steering vector samples construct a dictionary matrix:

$$\mathbf{A}_t = [\mathbf{a}(\varphi_1, \theta_1), \mathbf{a}(\varphi_2, \theta_2), \dots, \mathbf{a}(\varphi_{N_{dict}}, \theta_{N_{dict}})].$$
 (18)

The problem (17) can be rewritten as

$$\underset{\left\{\tilde{\mathbf{F}}_{\mathrm{BB},k}\right\}_{k=1}^{N_{f}}}{\operatorname{arg\,min}} \sum_{k=1}^{N_{f}} \left\|\mathbf{F}_{k}^{\mathrm{UC}} - \mathbf{A}_{t}\tilde{\mathbf{F}}_{\mathrm{BB},k}\right\|_{F}, \tag{19}$$
s.t.
$$\left\|\sum_{k=1}^{N_{f}} \left(\operatorname{diag}\left(\tilde{\mathbf{F}}_{\mathrm{BB},k}\tilde{\mathbf{F}}_{\mathrm{BB},k}^{H}\right)\right)\right\|_{0} = N_{\mathrm{RF}}, \tag{20}$$

$$\left\|\mathbf{A}_{t}\tilde{\mathbf{F}}_{\mathrm{BB},k}\right\|_{F}^{2} \leq \left\|\mathbf{F}_{k}^{\mathrm{UC}}\right\|_{F}^{2}, \forall k, \tag{21}$$

where $\tilde{\mathbf{F}}_{\mathrm{BB},k} \in \mathbb{C}^{N_{dict} \times N_a}$ is an auxiliary variables matrix. We obtain \mathbf{F}_{RF} and $\mathbf{F}_{\mathrm{BB},k}$ from \mathbf{A}_t and $\tilde{\mathbf{F}}_{\mathrm{BB},k}$. The constraint in (20) restricts $\tilde{\mathbf{F}}_{\mathrm{BB},k}$ to have only N_{RF} rows with non-zero elements, which implies that only N_{RF} steering vectors are selected from \mathbf{A}_t .

The problem (17) is reformulated as a standard sparsity-constrained matrix reconstruction problem (19), which can be solved using OMP. To solve the problem in (19), we extend the spatially sparse precoding algorithm in [24] to Algorithm 1. The algorithm begins with the first subband,

Algorithm 1 Wideband Hybrid Precoding via Orthogonal Matching Pursuit (OMP)

```
Require: \{\mathbf{F}_k^{\mathrm{UC}}\}_{k=1}^{N_f}, \mathbf{A}_t, N_{\mathrm{RF}}, N_t
1: for k=1,\ldots,N_f do
                                     if k = 1 then
      2:
                                                      \begin{split} \mathbf{F}_{\mathrm{RF}} &= \mathrm{zeros}(N_t, N_{\mathrm{RF}}) \\ \mathbf{F}_{res} &= \mathbf{F}_k^{\mathrm{UC}} \\ \text{for } i = 1, \dots, N_{\mathrm{RF}} \text{ do} \end{split}
      3:
      4:
       5:
                                                                          \Psi = \mathbf{A}_t^H \mathbf{F}_{res}
       6:
                                                                         m = \arg\max_{l=1,...,N_{dict}} (\mathbf{\Psi}\mathbf{\Psi}^H)_{l,l}
        7:
                                                                      egin{align*} m &= & \operatorname{arg\,litex}_{l=1,...,N_{dict}}(\mathbf{F}\mathbf{F}) \\ \mathbf{F}_{\mathrm{RF}}^{(i)} &= & \mathbf{A}_{t}^{(m)} \\ \mathbf{F}_{\mathrm{BB},k} &= & \left(\mathbf{F}_{\mathrm{RF}}^{H}\mathbf{F}_{\mathrm{RF}}\right)^{-1}\mathbf{F}_{\mathrm{RF}}^{H}\mathbf{F}_{k}^{\mathrm{UC}} \\ \mathbf{F}_{res} &= & \frac{\mathbf{F}_{k}^{\mathrm{UC}} - \mathbf{F}_{\mathrm{RF}}\mathbf{F}_{\mathrm{BB},k}}{\left\|\mathbf{F}_{k}^{\mathrm{UC}} - \mathbf{F}_{\mathrm{RF}}\mathbf{F}_{\mathrm{BB},k}\right\|_{F}} \end{aligned}
       8:
       9:
   10:
   11:
                                     else
   12:
                                                        \mathbf{F}_{\mathrm{BB},k} = \left(\mathbf{F}_{\mathrm{RF}}^H \mathbf{F}_{\mathrm{RF}}\right)^{-1} \mathbf{F}_{\mathrm{RF}}^H \mathbf{F}_k^{\mathrm{UC}}
   13:
   14:
   15: end for
  16: return \mathbf{F}_{\mathrm{RF}}, \{\mathbf{F}_{\mathrm{BB},k}\}_{k=1}^{N_f}
```

k=1. The projection of the unconstrained precoder $\mathbf{F}_{k=1}^{\mathrm{UC}}$ on the dictionary matrix \mathbf{A}_t is computed, then the steering vector $\mathbf{a}(\varphi_l,\theta_l), 1 \leq l \leq N_{dict}$ with highest projection is selected. The algorithm inserts the steering into the \mathbf{F}_{RF} . The $\mathbf{F}_{\mathrm{BB},k=1}$ is calculated by least square solutions, and the \mathbf{F}_{res} is updated by removing the contribution of the selected vector. It continues until the N_{RF} steering vectors are selected. For the next subband $k=2,\ldots,N_f$, the $\mathbf{F}_{\mathrm{BB},k}$ is computed using the least squares solution using the \mathbf{F}_{RF} obtained from the first subband. The algorithm returns \mathbf{F}_{RF} and $\{\mathbf{F}_{\mathrm{BB},k}\}_{k=1}^{N_f}$ as the final output.

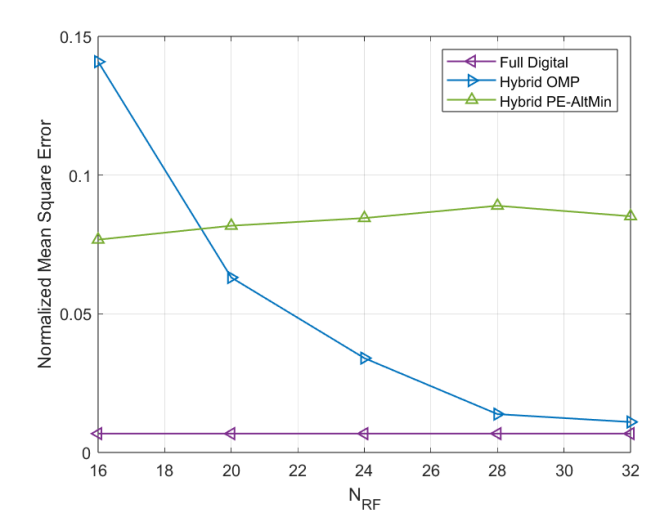


Fig. 2. The normalized mean square error vs. N_{RF} , $N_t = 128$.

IV. SIMULATION RESULTS

In this section, we evaluate the performance of our proposed algorithm using a practical 3GPP channel model. We adopt the CDL-A channel model [25] with 23 clusters and 20 paths for each cluster. The delay spread is 300 ns, and the maximum Doppler shift is 9.72 Hz. We consider a frequency center at 3.5 GHz. The subcarrier spacing is 30 kHz, and the number of subbands is $N_f=25$. We consider a single-polarization antenna in the BS and the UE. The number of UEs (N_u) is 4 with $N_r=2$ for each UE. Each UE antenna needs N_a coefficients to feed back. We set the number of CSI-RS antenna ports as $N_a=16$. The number of steering vectors in the dictionary matrix is $N_{dict}=1000$.

Fig. 2 shows the impact of the number of RF chains on the accuracy of the CSI feedback in normalized mean square error (NMSE) with BS antennas $N_t=128$. The NMSE is computed as

$$NMSE = \mathbb{E}\left\{\frac{\|\underline{\mathbf{H}} - \underline{\hat{\mathbf{H}}}\|_F^2}{\|\underline{\mathbf{H}}\|_F^2}\right\},\tag{22}$$

averaged over time, frequency, and number of UEs. NMSE performance is evaluated with different numbers of $N_{\rm RF} \in [16,32]$. The figure compares the proposed hybrid OMP method with the full digital method and the hybrid phase extraction alternating minimization (PE-AltMin) method [26]. The NMSE for the proposed hybrid OMP method approaches that of full digital precoding as $N_{\rm RF}$ increases, whereas the hybrid PE-AltMin remains relatively constant.

We evaluate spectral efficiency using zero forcing (ZF) precoding [27] derived from the estimated CSI. Each UE receives two data streams. For fair evaluation and simplicity, we assume that the ZF precoding is implemented in fully digital precoding. For a more realistic scenario, a hybrid precoding algorithm should be used to evaluate the spectral efficiency.

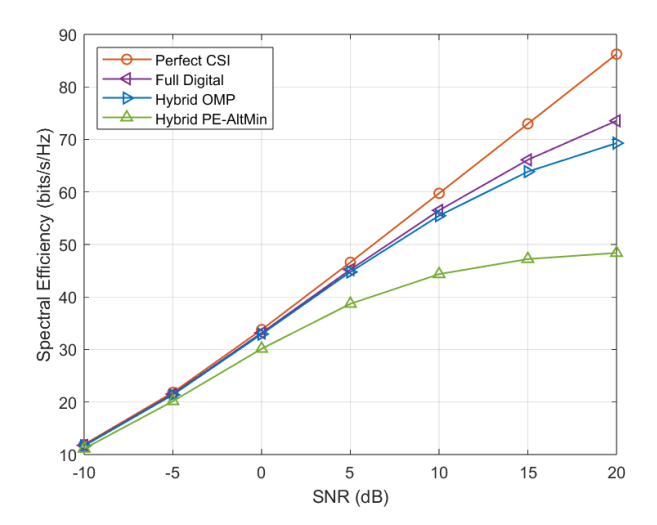


Fig. 3. The spectral efficiency vs. SNR, $N_t = 128$.

The spectral efficiency when $N_t=128$ and $N_{\rm RF}=32$ is shown in Fig. 3. The spectral efficiency is computed as

$$\sum_{u=1}^{N_u} \log_2(1 + SINR_u), \tag{23}$$

averaged over time and frequency, where SINR_u is the signal-to-interference-plus-noise ratio for the u-th UE. The figure shows that the performance of hybrid precoding is close to the full digital precoding. The unconstrained partial channel reciprocity precoding achieves high spectral efficiency with a reasonable amount of feedback $2N_a$ [19]. The proposed hybrid precoding algorithm reduces the number of RF chains (N_{RF}) while maintaining performance, making massive MIMO implementation more practical, even with a large number of BS antennas.

Finally, we investigate the impact of the size of the dictionary matrix. Fig. 4 shows the spectral efficiency for N_{dict} values of 400, 700, and 1000. The hybrid OMP algorithm selects the analog precoder vector from a set of steering vectors in the dictionary matrix. The spectral efficiency is better with a larger number of steering vector samples.

V. CONCLUSION

In this paper, we have proposed a codebook design for wideband FDD massive MIMO hybrid precoding systems. First, we derived the unconstrained partial channel reciprocity precoding that compresses the number of CSI feedback coefficients. We approximated the unconstrained precoding as a sparsityconstrained matrix reconstruction problem. We then designed wideband hybrid precoding using the OMP algorithm to find the optimal hybrid precoding. We presented simulation results that show the hybrid precoding achieved a performance close to that of the unconstrained precoding. In the future, we will evaluate the performance of a wideband massive MIMO hybrid precoding system with the proposed CSI feedback method

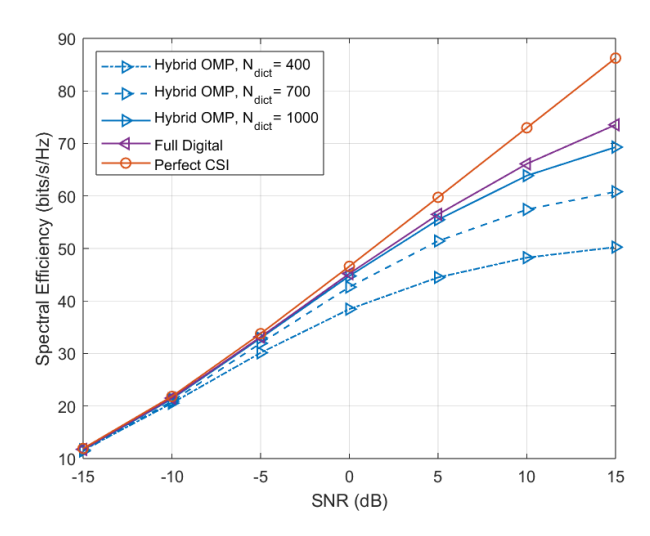


Fig. 4. The spectral efficiency vs. SNR with different sizes of dictionary matrix, $N_t=128$.

to investigate the feasibility of implementing wideband FDD massive MIMO hybrid precoding systems.

REFERENCES

- C.-X. Wang et al., "On the road to 6G: Visions, requirements, key technologies, and testbeds," *IEEE Commun. Surveys Tuts.*, vol. 25, no. 2, pp. 905–974, 2023.
- [2] E.-K. Hong et al., "6G R&D vision: Requirements and candidate technologies," J. Commun. Netw., vol. 24, no. 2, pp. 232–245, 2022.
- [3] H. Ju et al., "On the design of parity-check polar codes," in Proc 2024 15th Int Conf. Inf. Commun. Technol. Convergence (ICTC), Jeju Island, Korea, Republic of, Sep. 2024, pp. 755–758.
- [4] S.-Y. Lee et al., "A modified code design for punctured polar codes," in Proc 2024 15th Int Conf. Inf. Commun. Technol. Convergence (ICTC), Jeju Island, Korea, Republic of, Sep. 2024, pp. 751–754.
- [5] H. Ju et al., "On improving the design of parity-check polar codes," IEEE Open J. Commun. Soc., vol. 5, pp. 5552–5566, 2024.
- [6] H.-Y. Kwak et al., "Boosted neural decoders: Achieving extreme reliability of LDPC codes for 6G networks," IEEE J. Sel. Areas Commun., vol. 43, no. 4, pp. 1089–1102, 2025.
- [7] Y. Liu, Y. Deng, A. Nallanathan, and J. Yuan, "Machine learning for 6G enhanced ultra-reliable and low-latency services," *IEEE Wireless Commun.*, vol. 30, no. 2, pp. 48–54, 2023.
- [8] T. Mahboob, S. Tariq Shah, M. Choi, S.-H. Kim, and M. Young Chung, "Multi-operator spectrum and MEC resource sharing in next generation cellular networks," *IEEE Access*, vol. 12, pp. 91634–91648, 2024.
- [9] M. Shin, D. Mehmood Mughal, S.-H. Kim, and M. Young Chung, "Deep reinforcement learning assisted multi-operator spectrum sharing in cellfree MIMO networks," *IEEE Commun. Lett.*, vol. 28, no. 12, pp. 2894– 2898, Dec. 2024.
- [10] E. G. Larsson, O. Edfors, F. Tufvesson, and T. L. Marzetta, "Massive MIMO for next generation wireless systems," *IEEE Commun. Mag.*, vol. 52, no. 2, pp. 186–195, Feb. 2014.
- [11] T. L. Marzetta, "Noncooperative cellular wireless with unlimited numbers of base station antennas," *IEEE Trans. Wireless Commun.*, vol. 9, no. 11, pp. 3590–3600, Nov. 2010.
- [12] X. Rao and V. K. N. Lau, "Distributed compressive CSIT estimation and feedback for FDD multi-user massive MIMO systems," *IEEE Trans. Signal Process.*, vol. 62, no. 12, pp. 3261–3271, Jun. 2014.
- [13] Y. Han, J. Lee, and D. J. Love, "Compressed sensing-aided downlink channel training for FDD massive MIMO systems," *IEEE Trans. Commun.*, vol. 65, no. 7, pp. 2852–2862, Jul. 2017.
- [14] C.-K. Wen, W.-T. Shih, and S. Jin, "Deep learning for massive MIMO CSI feedback," *IEEE Wireless Commun. Lett.*, vol. 7, no. 5, pp. 748–751, Oct. 2018.

- [15] Z. Lu, J. Wang, and J. Song, "Multi-resolution CSI feedback with deep learning in massive MIMO system," in *Proc. IEEE Int. Conf. Commun.* (ICC), Dublin, Ireland, Jun. 2020, pp. 1–6.
- [16] P. Liang, J. Fan, W. Shen, Z. Qin, and G. Y. Li, "Deep learning and compressive sensing-based CSI feedback in FDD massive MIMO systems," *IEEE Trans. Veh. Technol.*, vol. 69, no. 8, pp. 9217–9222, Aug. 2020.
- [17] A. Adhikary, J. Nam, J.-Y. Ahn, and G. Caire, "Joint spatial division and multiplexing—The large-scale array regime," *IEEE Trans. Inf. Theory*, vol. 59, no. 10, pp. 6441–6463, Oct. 2013.
- [18] M. Barzegar Khalilsarai, S. Haghighatshoar, X. Yi, and G. Caire, "Fdd massive MIMO via UL/DL channel covariance extrapolation and active channel sparsification," *IEEE Trans. Wireless Commun.*, vol. 18, no. 1, pp. 121–135, Jan. 2019.
- [19] H. Yin and D. Gesbert, "A partial channel reciprocity-based codebook for wideband FDD massive MIMO," *IEEE Trans. Wireless Commun.*, vol. 21, no. 9, pp. 7696–7710, Sep. 2022.
- [20] X. Zhang, L. Zhong, and A. Sabharwal, "Directional training for FDD massive MIMO," *IEEE Trans. Wireless Commun.*, vol. 17, no. 8, pp. 5183–5197, Aug. 2018.
- [21] W. Shen, L. Dai, B. Shim, Z. Wang, and R. W. Heath, "Channel feedback based on AoD-adaptive subspace codebook in FDD massive MIMO systems," *IEEE Trans. Commun.*, vol. 66, no. 11, pp. 5235–5248, Nov. 2018.
- [22] A. F. Molisch et al., "Hybrid beamforming for massive MIMO: A survey," IEEE Commun. Mag., vol. 55, no. 9, pp. 134–141, Sep. 2017.
- [23] L. Miretti, R. L. Cavalcante, and S. Stanczak, "FDD massive MIMO channel spatial covariance conversion using projection methods," in *Proc. IEEE Int. Conf. Acoust., Speech Signal Process. (ICASSP)*, Calgary, AB, Canada, Apr. 2018, pp. 3609–3613.
- [24] O. E. Ayach, S. Rajagopal, S. Abu-Surra, Z. Pi, and R. W. Heath, "Spatially sparse precoding in millimeter wave MIMO systems," *IEEE Trans. Wireless Commun.*, vol. 13, no. 3, pp. 1499–1513, Mar. 2014.
- [25] 3GPP, "5G; Study on channel model for frequencies from 0.5 to 100 GHz," Tech. Rep. TR 38.901, 2024. [Online]. Available: http://www.3gpp.org
- [26] X. Yu, J.-C. Shen, J. Zhang, and K. B. Letaief, "Alternating minimization algorithms for hybrid precoding in millimeter wave MIMO systems," *IEEE J. Sel. Topics Signal Process.*, vol. 10, no. 3, pp. 485–500, Apr. 2016.
- [27] C. Peel, B. Hochwald, and A. Swindlehurst, "A vector-perturbation technique for near-capacity multiantenna multiuser communication-part i: channel inversion and regularization," *IEEE Trans. Commun.*, vol. 53, no. 1, pp. 195–202, Jan. 2005.